RESEARCH ARTICLE

Data-Driven Predictive Control With Switched Subspace Matrices for an SCR System

JINGHUA ZHAO [1,2]**, JIE LIU**[1]**, HONGYU SUN**[1]**, YUNFENG HU** [2]**, YAO SUN** [2]**, AND FANGXI XIE**[2]

[1]Computer College, Jilin Normal University, Siping 136002, China
[2]State Key Laboratory of Automotive Simulation and Control, Jilin University, Changchun 130022, China

Corresponding author: Yao Sun (syao@jlu.edu.cn)

ABSTRACT Selective catalytic reduction (SCR) systems are distributed systems with strong time-varying parameter characteristics such that an accurate model for it is difficult to establish. Its control task simultaneously achieving high NO_x conversion efficiency and low NH_3 slip is a typical multi-objective and multi-constraint problem, which is suitable to be solved in the framework of the model predictive control (MPC). However, how to find a data-driven identification method based on the dynamic characteristics of an SCR system and a corresponding MPC method for satisfying its emission requirements remain a formidable challenge. The sufficient identification for the traditional identification method with fixed subspace model requires an excessively high order subspace matrix, such that a degradation in real-time performance is caused and the generality of the method under non-identification conditions is limited. In this paper, utilizing the transient data of the SCR system under the WHTC cycle, a novel identification method for some lower order subspace matrices excited by the segmented data referring to the dynamic of the ammonia coverage ratio is established. A corresponding predictive controller with the switched subspace matrices according to working conditions is designed in order to further improve its real-time performance, generality and robustness. The simulation results show that under the identification condition the proposed predictive controller compared to the traditional method can improve the emissions of NO_x and NH_3, that under the non-identification condition the proposed predictive controller can also improve the emissions and its optimization effects have better robustness to uncertainties of the transient cycle, and that the proposed predictive controller saves an significant computation time.

INDEX TERMS Subspace identification, data-driven predictive control, SCR systems.

I. INTRODUCTION

Selective catalytic reduction (SCR) systems are the most promising aftertreatment technologies for reducing the NO_x emission [1]. The working principle of SCR systems is that NO_x exhausted by engines can be reduced by ammonia (NH_3) generated from a 32.5% aqueous urea solution (AdBlue), and the excess NH_3 is also a harmful emission [2]. Therefore, the key to controlling SCR systems is how to improve the NO_x conversion rate while ensuring that the NH_3 slip does not exceed the limit. Researchers introduce ammonia coverage

rates in the modeling process and balance the NO_x and NH_3 emissions by optimizing them [3]. That is a typical multi-objective problem with constraints, which is suitable to be solved under the model predictive control (MPC) framework [4]. The working processes of SCR systems involve many complex chemical reactions and transfer processes of heat and mass. SCR systems are distributed systems with strong time-varying parameter characteristics such that an accurate system model for it is difficult to establish [5], [6].

In recent years, large amounts of data can be obtained in modern industries with the development of the computer technology. Modeling through data-driven methods not only becomes possible but also new challenges both in theory

---

The associate editor coordinating the review of this manuscript and approving it for publication was Haibin Sun.

and applications [7]. These data-based methods get around the difficulty of mechanism modeling. In addition, the MPC strategy takes time-domain constraints into account explicitly and deals with multiple objectives in a somewhat optimal sense, so it has a great potential for the control of an automated machinery [8]. In [9], a data-driven predictive control algorithm with elegantly combining data-driven subspace identification and MPC is proposed.

The data-driven technology has been widely used in industrial occasions such as multidimensional blast furnace system, wind power generation, vapor compression refrigeration cycle and superheated steam temperature system in power plant. In [10], a data-driven model based on Volterra series is developed for multidimensional blast furnace system. Three different low-order Volterra filters are designed to effectively describe the evolution of the studied silicon sequence. In [11], based on the data-driven technology, a predictive controller of wind turbine torque is designed. The engine torque is controlled by the prediction of wind force to change the rotation speed, so as to obtain the best power coefficient and maximize the power. And different data mining algorithms are used to improve the accuracy and robustness properties of the wind speed model. In [12], a controller of vapor compression refrigeration cycle system driven by multivariable data is proposed, which controls the opening of expansion valve to realize the overheating of evaporator and constant pressure. The controller shows satisfactory robustness to the disturbance caused by the change of temperature variable. In [13], a pre-set adaptive predictive controller using the data-driven technology for superheated steam temperature system in power plant is designed, which shows strong anti-interference ability and desirable robustness in off-design system.

Moreover, the data-driven technology has been used in many aspects of vehicle mechanical components control. In [14], a torque coordination controller of hybrid electric vehicle (HEV) drive system based on a data-driven method is proposed. Excellent quality in the dynamic process of HEV mode switching from pure electric to hybrid drive is achieved by the controller, which can significantly improve the driver comfort and economy of HEV. In addition, the latest vehicle operation data collected online can be used to update the subspace prediction model for ensuring the higher performance of the proposed control strategy for a long time. In [15], an air-fuel ratio controller for the engine is designed by using the data-driven technology to achieve small air-fuel ratio error, reasonable injection duration and injection pulse width increment. It remains effective in real-time simulation experiments with interference. In [16], a combustion controller for the diesel engine is designed by using the data-driven technology with the system matrix put forward from the kernel function to realize the real-time coordinated control of power and emission. In [17], a data-driven predictive controller for the starting process of automatic manual transmission (AMT) vehicle is designed to obtain satisfied startup performance by controlling slip speed of the clutch. In [18], a shift controller

is designed with the data-driven predictive control technology to improve the shift quality of dual clutch transmission (DCT) vehicles. The controller is robust to the disturbance caused by the uncertainty of working conditions.

Additionally, researchers have made considerable efforts to solve the problems of the modeling and optimal control for SCR systems utilizing the data-driven technology during recent years. In [19], a urea dosing controller of the SNCR denitration system based on the data-driven technology is designed, which strictly controls the concentration of NO_x at the outlet of the SNCR. The experimental results show that the fluctuation of the concentration of NO_x at the outlet is relatively gentle, and the ammonia dosing amount and ammonia escape amount are generally reduced. In [20], a data-driven method is used to establish the NO_x model at the outlet of an SCR system, and an optimal control strategy of urea dosing is proposed, which can ensure the denitration efficiency and reduce the ammonia escape when the working conditions change. In [21], a fixed subspace matrix and a data-driven model using the engine data of the ETC transient cycle are identified, and a urea dosing controller is designed. Thus, Utilizing the experimental data of commercial SCR systems, a data-driven subspace model can be established to avoid the problem of mechanistic modeling and a corresponding MPC method can also solve their problem of emission optimization.

Overall, there are many researches on the data-driven technology applied to SCR systems, most of which are based on the traditional identification method with fixed subspace model, and the dynamic characteristics of SCR systems are rarely considered in the identification process. Compared to the traditional identification method and corresponding MPC method, there are several challenges in the development of a data-driven predictive controller for SCR systems:

1). How to find a data-driven identification method based on the dynamic characteristics of an SCR system and a corresponding MPC method for satisfying its emission requirements remain a formidable challenge.

2). The sufficient identification for the traditional identification method with fixed subspace model requires an excessively high order subspace matrix, such that a degradation in real-time performance is caused and the generality of the method under non-identification conditions is limited.

To address the associated challenges as mentioned above, the primary merits of the design procedure cover the following points:

1). A novel identification method for some lower order subspace matrices excited by the segmented data referring to the dynamic of the ammonia coverage ratio is established.

2). A corresponding predictive controller with the switched subspace matrices according to working conditions is designed in order to further improve the real-time performance, generality and robustness.

The rest of this paper is organized as follows. Section 1 explains the problem statement of the SCR system. Section 2 presents the traditional data-driven predictive

controller with fixed subspace identification model. Section 3 primarily elaborates the proposed data-driven predictive controller with segmented subspace identification model and shows its optimization results. Section 4 presents the conclusion.

II. PROBLEM STATEMENT OF SCR SYSTEM

SCR systems are complex dynamic systems of chemical reaction with highly nonlinear properties. Their chemical reaction primarily includes the following several processes. The AdBlue ($Urea_{in}$) is pyrolyzed to produce ammonia ($NH_{3,in}$) and isocyanate (HNCO) at the upstream of an SCR system. Inside the catalyst, one part of $NH_{3,in}$ is adsorbed on the catalyst substrate ($NH_3(ads)$), while the other part remains in the gaseous phase ($NH_3(g)$). Both parts can be transformed into each other, i.e.,

$$NH_3(ads) \leftrightarrow NH_3(g). \tag{1}$$
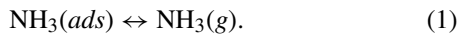
The $NH_3(ads)$ can catalytically react with the $NO_x(NO_{x,in})$ generated by the engine, and then they are converted into N_2 and H_2O. When the temperature is higher than 200 degrees Celsius, the SCR system is governed by an Eley-Rideal mechanism [22] consuming $NH_3(ads)$ and gaseous NO_x,

$$4NH_3(ads) + 4NO_x + zO_2 \rightarrow 4N_2 + 6H_2O. \tag{2}$$
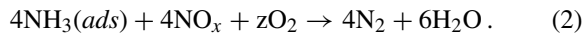
The $NH_3(ads)$ can also be oxidized to N_2 and H_2O by the following reaction:

$$4NH_3(ads) + 3O_2 \rightarrow 2N_2 + 6H_2O. \tag{3}$$
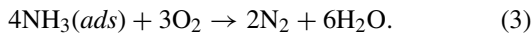
Proceeding through the chemical reaction described above, the remaining NO_x ($NO_{x,out}$) and NH_3 ($NH_{3,out}$) are discharged as pollutants. The ratio of the amount of $NH_3(ads)$ and the ammonia storage capacity is defined as the ammonia coverage ratio θ_{NH_3}.

A schematic diagram of problem statement for an SCR system is shown in Fig. 1. For the SCR system, the primary inputs are $NO_{x,in}$, $NH_{3,in}$, EF_M (the exhaust gas mass flow) and T_{engine} (the exhaust gas temperature of engine), and the primary outputs are $NO_{x,out}$ and $NH_{3,out}$, and the primary internal state is θ_{NH_3}. The control task of the SCR system is to simultaneously achieve high NO_x conversion efficiency (the ratio of ($NO_{x,in} - NO_{x,out}$) to $NO_{x,in}$) and low ammonia slip $NH_{3,out}$. The task can be achieved through the optimization and tracking control of θ_{NH_3}, which is used to balance the NO_x and NH_3 emissions [2, 3].
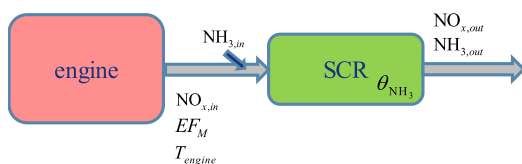

FIGURE 1. Schematic of the problem statement for the SCR system.

III. TRDAIONAL DATA-DRIVEN PREDICTIVE CONTROLLER

In this section, a traditional data-driven predictive controller with fixed subspace identification model is designed and

verified for an SCR system. Firstly, a subspace identification model and an incremental subspace identification model are presented. Secondly, a traditional data-driven predictive controller is proposed. Thirdly, a few simulations are performed to verify the traditional data-driven predictive controller with fixed subspace identification model under the WHTC cycle. Finally, the computation times of the data-driven predictive controllers between the different order subspace matrices are compared and discussed.

A. SUBSPACE IDENTIFICATION MODEL

According to the problem statement of SCR systems, a state-space model with discretized form considered for deriving the subspace matrices is presented as follows:

$$\begin{cases} x(k+1) = Ax(k) + B_u u(k) + Kd(k), \\ y_c(k) = Cx(k), \\ y_b(k) = C_b x(k), \end{cases} \tag{4}$$

which is a system with four inputs and two outputs, the control input $u(k) = NH_{3,in}$, the control output $y^c(k) = NO_{x,out}$, the system constrained output $y^b(k) = NH_{3,out}$ and the disturbance input $d(k)$ is constructed as follows:

$$d(k) = \begin{bmatrix} d^1(k) & d^2(k) & d^3(k) \end{bmatrix}^T = \begin{bmatrix} NO_{x,in} & EF_M & T_{engine} \end{bmatrix}.$$

The state of the system is $x(k) \in \mathbb{R}^n$ (n is the state order), and the matrices A, B_u, K, C, C_b are the state-space matrices. The data of $u(k)$, $d(k)$, $y^c(k)$ and $y^b(k)$ for $k \in \{0, 1, \cdots, 2i+j-1\}$ are collected through the high-precision model of an SCR system. The prediction horizon and the control horizon are denoted as N_p and N_u, satisfying $N_p \geq N_u$. The number of counting elements are denoted as j with $i = Np$. The data block Hankel matrices U_p, U_f, Y_p and Y_f are constructed as follows:

$$U_p = \begin{bmatrix} u_0 & u_1 & \cdots & u_{j-1} \\ d_0^1 & d_1^1 & \cdots & d_{j-1}^1 \\ d_0^2 & d_1^2 & \cdots & d_{j-1}^2 \\ d_0^3 & d_1^3 & \cdots & d_{j-1}^3 \\ u_1 & u_2 & \cdots & u_j \\ d_1^1 & d_2^1 & \cdots & d_j^1 \\ \vdots & \vdots & & \vdots \\ u_{i-1} & u_{2i} & \cdots & u_{i+j-2} \\ d_{i-1}^1 & d_{2i}^1 & \cdots & d_{i+j-2}^1 \\ d_{i-1}^2 & d_{2i}^2 & \cdots & d_{i+j-2}^2 \\ d_{i-1}^3 & d_{2i}^3 & \cdots & d_{i+j-2}^3 \end{bmatrix}_{4i \times j},$$

$$U_f = \begin{bmatrix} u_i & u_{i+1} & \cdots & u_{i+j-1} \\ d_i^1 & d_{i+1}^1 & \cdots & d_{i+j-1}^1 \\ d_i^2 & d_{i+1}^2 & \cdots & d_{i+j-1}^2 \\ d_i^3 & d_{i+1}^3 & \cdots & d_{i+j-1}^3 \\ u_{i+1} & u_{i+2} & \cdots & u_{i+j} \\ d_{i+1}^1 & d_{i+2}^1 & \cdots & d_{i+j}^1 \\ \vdots & \vdots & & \vdots \\ u_{2i-1} & u_{2i} & \cdots & u_{2i+j-2} \\ d_{2i-1}^1 & d_{2i}^1 & \cdots & d_{2i+j-2}^1 \\ d_{2i-1}^2 & d_{2i}^2 & \cdots & d_{2i+j-2}^2 \\ d_{2i-1}^3 & d_{2i}^3 & \cdots & d_{2i+j-2}^3 \end{bmatrix}_{4i \times j},$$

$$Y_p = \begin{bmatrix} y_0^c & y_1^c & \cdots & y_{j-1}^c \\ y_0^b & y_1^b & \cdots & y_{j-1}^b \\ y_1^c & y_2^c & \cdots & y_j^c \\ y_1^b & y_2^b & \cdots & y_j^b \\ \vdots & \vdots & & \vdots \\ y_{i-1}^c & y_i^c & \cdots & y_{i+j-2}^c \\ y_{i-1}^b & y_i^b & \cdots & y_{i+j-2}^b \end{bmatrix}_{2i \times j},$$

$$Y_f = \begin{bmatrix} y_i^c & y_{i+1}^c & \cdots & y_{i+j-1}^c \\ y_i^b & y_{i+1}^b & \cdots & y_{i+j-1}^b \\ y_{i+1}^c & y_{i+2}^c & \cdots & y_{i+j}^c \\ y_{i+1}^b & y_{i+2}^b & \cdots & y_{i+j}^b \\ \vdots & \vdots & & \vdots \\ y_{2i-1}^c & y_{2i}^c & \cdots & y_{2i+j-2}^c \\ y_{2i-1}^b & y_{2i}^b & \cdots & y_{2i+j-2}^b \end{bmatrix}_{2i \times j},$$

where p and f denote the past and future block observations. According to the deviation of the subspace linear predictor presented in literature [23], we will recursively develop the subspace input–output matrix equation in the field of subspace identification. The prediction Eq. (5) for subspace identification is obtained by recursive method [24].

$$\hat{Y}_f = L_w W_p + L_u U_f, \tag{5}$$

where

$$W_p = \begin{bmatrix} Y_p \\ U_p \end{bmatrix}_{6i \times j}$$

and subspace matrices L_w and L_u are obtained by finding the prediction of future output Y_f and by solving the following least squares problem:

$$\min_{L_w, L_u} \left\| Y_f - \begin{bmatrix} L_w & L_u \end{bmatrix} \begin{bmatrix} W_p \\ U_f \end{bmatrix} \right\|^2. \tag{6}$$

The solution is the orthogonal projection of the row space of Y_f into the row space spanned by W_f and U_f as [25]:

$$L_{wu} = \begin{bmatrix} L_w & L_u \end{bmatrix} = Y_f \begin{bmatrix} W_p \\ U_f \end{bmatrix}^{\dagger}$$

$$= Y_f \begin{bmatrix} W_p^T & U_f^T \end{bmatrix} \left(\begin{bmatrix} W_p \\ U_f \end{bmatrix} \begin{bmatrix} W_p^T & U_f^T \end{bmatrix} \right)^{-1}, \tag{7}$$

where $\dagger$ represents the Moore–Penrose pseudoinverse. In terms of (6) and (7), we can obtain subspace matrices L_w and L_u as follow:

$$L_w = [L_{wu}(:,1), \cdots, L_{wu}(:, N_P \times 6)]_{2N_P \times 6N_P},$$
$$L_u = [L_{wu}(:, N_P \times 6 + 1), \cdots, L_{wu}(:, N_P \times 10)]_{2N_P \times 4N_P}.$$

In order to simplify the derivation of the predictive controller and reduce the computation time, the first column of $\hat{Y}_f$ is only used to predict the future dynamics of the system:

$$\hat{y}_f = L_w w_p + L_u u_f \tag{8}$$

where

$$w_p = \begin{bmatrix} y_p \\ u_p \end{bmatrix},$$

$$u_p = \begin{bmatrix} u(k - N_u + 1) \\ d^1(k - N_u + 1) \\ d^2(k - N_u + 1) \\ d^3(k - N_u + 1) \\ u(k - N_u + 2) \\ d^1(k - N_u + 2) \\ \vdots \\ u(k) \\ d^1(k) \\ d^2(k) \\ d^3(k) \end{bmatrix}_{4N_u \times 1}, \quad u_f = \begin{bmatrix} u(k + 1) \\ d^1(k + 1) \\ d^2(k + 1) \\ d^3(k + 1) \\ u(k + 2) \\ d^1(k + 2) \\ \vdots \\ u(k + N_u) \\ d^1(k + N_u) \\ d^2(k + N_u) \\ d^3(k + N_u) \end{bmatrix}_{4N_u \times 1},$$

$$y_p = \begin{bmatrix} y^c(k - N_p + 1) \\ y^b(k - N_p + 1) \\ y^c(k - N_p + 2) \\ y^b(k - N_p + 2) \\ \vdots \\ y^c(k) \\ y^b(k) \end{bmatrix}_{2N_p \times 1}, \quad \hat{y}_f = \begin{bmatrix} y^c(k + 1) \\ y^b(k + 1) \\ y^c(k + 2) \\ y^b(k + 2) \\ \vdots \\ y^c(k + N_p) \\ y^b(k + N_p) \end{bmatrix}_{2N_p \times 1}.$$

Since the disturbance of the system is unpredictable, it is assumed to be constant in the prediction horizon. Extracting the disturbance from the control input, Eq. (8) can be expressed as:

$$\hat{y}_f = \tilde{L}_w \tilde{w}_p + L_d^p d_p + \tilde{L}_u \tilde{u}_f + L_d^f d_f. \tag{9}$$

B. INCREMENTAL SUBSPACE IDENTIFICATION MODEL

In order to guarantee zero steady-state error for the tracking of the system output to the reference input, an integral form is introduced. The Eq. (9) is transformed into an incremental form:

$$\Delta \hat{y}_f = \tilde{L}_w \Delta \tilde{w}_p + L_d^p \Delta d_p + \tilde{L}_u \Delta \tilde{u}_f + L_d^f \Delta d_f. \tag{10}$$

Assuming that the future disturbance input d_f is unchanged in the control horizon, the incremental form of the predicted output sequence at the k sampling time is:

$$\Delta \overset{\wedge}{\underset{f}{y}}(k) = \tilde{L}_{wI}\left(1:N_P,:\right)\begin{bmatrix}\Delta y_p\\\Delta \tilde{u}_p\end{bmatrix}$$
$$+ L_{dI}^p\left(1:N_p,:\right)\Delta d_p$$
$$+ L_{dI}^f\left(1:N_p,:\right)\Delta d_f$$
$$+ L_{uI}^f\left(1:N_p,1:N_u\right)\Delta \tilde{u}_f(k), \quad (11)$$

where

$$\tilde{L}_{wI} = \Pi \tilde{L}_w, \ L_{dI}^p = \Pi L_d^p, \ L_{dI}^f = \Pi L_d^f, \ \tilde{L}_{uI} = \Pi L_u,$$
$$\Delta y_p = \begin{bmatrix}\Delta y(k-N_p+1) \ \Delta y(k-N_p+2) \ \cdots \ \Delta y(k)\end{bmatrix}^T,$$
$$\Delta \tilde{u}_p = \begin{bmatrix}\Delta u(k-N_p) \ \Delta u(k-N_p+1) \ \cdots \ \Delta y(k-1)\end{bmatrix}^T,$$
$$\Delta d_p = \begin{bmatrix}\Delta d(k-N_p+1) \ \Delta d(k-N_u+2) \ \cdots \ \Delta d(k)\end{bmatrix}^T,$$
$$\Delta d_p = \begin{bmatrix}\Delta d(k) \ 0 \ \cdots \ 0\end{bmatrix}^T,$$
$$\Pi = \begin{bmatrix}I & 0 & \cdots & 0\\I & I & \cdots & 0\\\vdots & \vdots & & 0\\I & I & \cdots & I\end{bmatrix}_{2N_p\times 2N_p}.$$

To design a data-driven predictive controller with constraints, the incremental predicted outputs shown in Eq. (11) are accumulated. The predicted control output $\hat{y}_f^c$ and the predicted constraint output $\hat{y}_f^b$ are further extracted from $\hat{y}_f$ as:

$$\begin{cases}\Delta \hat{y}_f^c(k) = \Gamma_c \Delta \hat{y}_f(k)\\\Delta \hat{y}_f^b(k) = \Gamma_b \Delta \hat{y}_f(k),\end{cases} \quad (12)$$

where

$$\Gamma_c = \begin{bmatrix}1 & 0 & 0 & 0 & 0 & \cdots & 0 & 0\\0 & 0 & 1 & 0 & 0 & \cdots & 0 & 0\\\vdots & \vdots & \vdots & \vdots & \vdots & & \vdots & \vdots\\0 & 0 & 0 & 0 & 0 & \cdots & 1 & 0\end{bmatrix}_{N_p\times 2N_p},$$
$$\Gamma_b = \begin{bmatrix}0 & 1 & 0 & 0 & 0 & \cdots & 0 & 0\\0 & 0 & 0 & 1 & 0 & \cdots & 0 & 0\\\vdots & \vdots & \vdots & \vdots & \vdots & & \vdots & \vdots\\0 & 0 & 0 & 0 & 0 & \cdots & 0 & 1\end{bmatrix}_{N_p\times 2N_p}.$$

In Eq. (12), the predicted control output and the predicted constraint output are

$$\begin{cases}\hat{y}_f^c(k+1) = F^c + S_f^c \Delta \tilde{u}_f(k)\\\hat{y}_f^b(k+1) = F^b + S_f^b \Delta \tilde{u}_f(k),\end{cases} \quad (13)$$

where

$$\begin{cases}F^c = y^c(k) + \Gamma_c \tilde{L}_{wI}\left(1:N_p,:\right)\begin{bmatrix}\Delta y_p\\\Delta \tilde{u}_p\end{bmatrix}\\\qquad + \Gamma_c L_{dI}^p\left(1:N_p,:\right)\Delta d_p\\\qquad + \Gamma_c L_{dI}^f\left(1:N_p,1:N_u\right)\Delta d_f\\F^b = y^b(k) + \Gamma_b \tilde{L}_{wI}\left(1:N_p,:\right)\begin{bmatrix}\Delta y_p\\\Delta \tilde{u}_p\end{bmatrix}\\\qquad + \Gamma_b L_{dI}^p\left(1:N_p,:\right)\Delta d_p\\\qquad + \Gamma_b L_{dI}^f\left(1:N_p,1:N_u\right)\Delta d_f,\end{cases}$$
$$\begin{cases}S_f^c = \Gamma_c \tilde{L}_{uI}\left(1:N_p,1:N_u\right)\\S_f^b = \Gamma_b \tilde{L}_{uI}\left(1:N_p,1:N_u\right),\end{cases}$$
$$\begin{cases}y^c(k) = \begin{bmatrix}y^c(k)\\y^c(k)\\\vdots\\y^c(k)\end{bmatrix}_{N_p\times 1}\\y^b(k) = \begin{bmatrix}y^b(k)\\y^b(k)\\\vdots\\y^b(k)\end{bmatrix}_{N_p\times 1},\end{cases}$$

where F^c and F^b are the system free response, and S_f^c and S_f^b are the system control response.

C. TRADITIONAL DATA-DRIVEN PREDICTIVE CONTROLLER WITH INCREMENTED SUBSPACE IDENTIFICATION MODEL

In this subsection, a data-driven predictive controller with incremental subspace identification model is developed to account for the emission objectives and constraints and optimize $NH_{3,in}$ for the SCR system, as shown in Fig. 2.
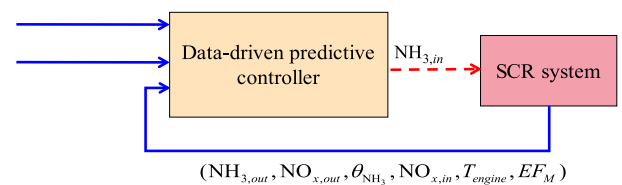

FIGURE 2. Schematic of data-driven predictive controller for optimizing $NH_{3,in}$.

The key to controlling SCR systems is how to improve the NO_x conversion rate while ensuring that the NH_3 slip does not exceed the limit. Thus, the optimization problem with the input and output constraints of the SCR system is described as follows:

$$\min_{\Delta u_f(k)} J\left(y_f^c(k), \Delta u_f(k), N_p, N_u\right), \quad (14)$$

where

$$J = \left[R_e(k+1) - F^c - S^c \Delta \tilde{u}_f(k)\right]^T$$
$$\times \left[R_e(k+1) - F^c - S \Delta \tilde{u}_f(k)\right]$$
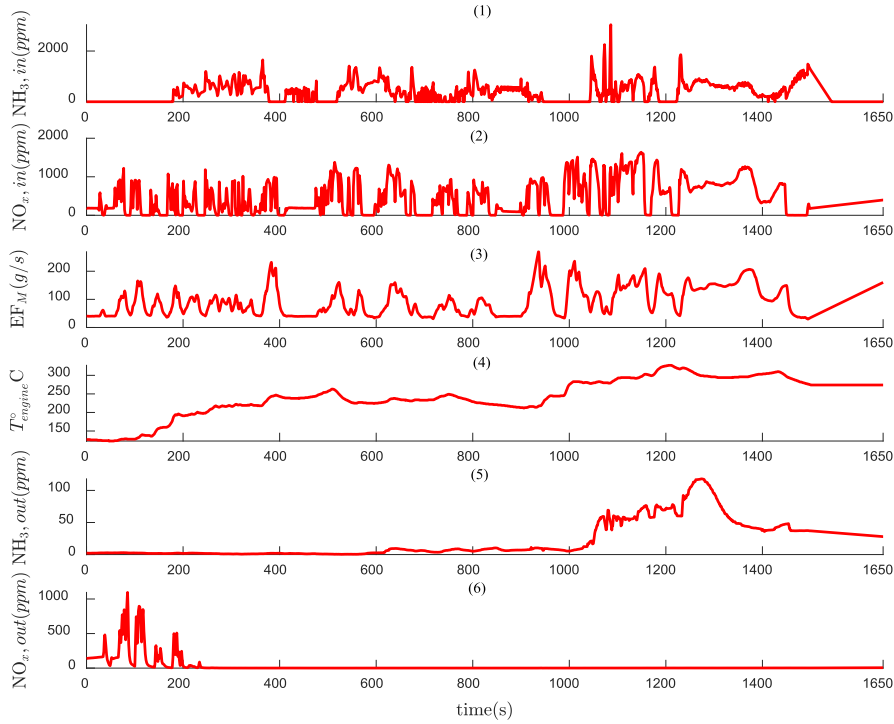$$+ \Delta \tilde{u}_f(k)^T (\Lambda I) \Delta \tilde{u}_f(k),$$

FIGURE 3. Input and output data of the SCR system under the WHTC cycle with cold-initial engine.

$$u_{\min}(k+q) \le u(k+q) \le u_{\max}(k+q),$$
$$\Delta u_{\min}(k+q) \le \Delta u(k+q) \le \Delta u_{\max}(k+q),$$
$$y_{\min}^b(k+m) \le \hat{y}^b(k+q) \le y_{\max}^b(k+m),$$
$$\Lambda = \Gamma_u / \Gamma_y,$$

$$\Gamma_y = \begin{bmatrix} \gamma_{y,1} & 0 & \cdots & 0 \\ 0 & \gamma_{y,2} & \cdots & 0 \\ \vdots & \vdots & & \vdots \\ 0 & 0 & \cdots & \gamma_{y,N_p} \end{bmatrix},$$

$$\Gamma_u = \begin{bmatrix} \gamma_{u,1} & 0 & \cdots & 0 \\ 0 & \gamma_{u,2} & \cdots & 0 \\ \vdots & \vdots & & \vdots \\ 0 & 0 & \cdots & \gamma_{u,N_u} \end{bmatrix}. \quad (15)$$

The optimization function J consists of two parts: the predictive control output $\hat{y}_f^c(k+1)$ tracks the desired reference value ($R_e(k+1)$); the change rate of the control action $\Delta u_f(k)$ is as small as possible. Because of the physical constraints of the SCR system, the range of control input $u(k)$ and constraint output $y^b(k)$ are: $u_{\min} = \Delta u_{\min} = 0 \, mol/s$, $u_{\max} = 0.003 \, mol/s$, $\Delta u_{\max} = 0.0005 \, mol/s$, $y_{\min}^b = 0 \, mol/s$ and $y_{\max}^b = 0.00002 \, mol/s$. The weight factor matrices Γ_u and Γ_y are given to trade off the two objectives. The ratio of weight coefficient Γ_u and Γ_y is Λ.

Since problem (15) is a multi-objective optimization problem with constraints [26], [27], the efficient set method can be used to solve it [28]. In order to facilitate the solution by the efficient set method, the relevant constraints can be

organized as:

$$A\Delta\tilde{u}_f \le b, \quad (16)$$

where

$$A = \begin{bmatrix} -I \\ -R \\ -S^b \\ I \\ R \\ S^b \end{bmatrix}_{6N_p \times N_u}, \quad b = \begin{bmatrix} -L_1 \\ -L_2 \\ -L_3 \\ U_1 \\ U_2 \\ U_3 \end{bmatrix}_{6N_p \times 1},$$

$$L_1 = \begin{bmatrix} \Delta u_{min}(k) & \cdots & \Delta u_{min}(k+q+1) \end{bmatrix}^T,$$
$$U_1 = \begin{bmatrix} \Delta u_{max}(k) & \cdots & \Delta u_{max}(k+q+1) \end{bmatrix}^T,$$
$$L_2 = \begin{bmatrix} u_{min}(k)-u(k-1) & \cdots & u_{min}(k+q-1)-u(k-1) \end{bmatrix}^T,$$
$$U_2 = \begin{bmatrix} u_{max}(k)-u(k-1) & \cdots & u_{max}(k+q-1)-u(k-1) \end{bmatrix}^T,$$
$$L_3 = \begin{bmatrix} y_{min}^b(k+1) & \cdots & y_{min}(k+m) \end{bmatrix}^T - F^b,$$
$$U_3 = \begin{bmatrix} y_{max}^b(k+1) & \cdots & y_{max}(k+m) \end{bmatrix}^T - F^b,$$

$$I = \begin{bmatrix} 1 & 0 & \cdots & 0 \\ 0 & 1 & \cdots & 0 \\ \vdots & \vdots & & \vdots \\ 0 & 0 & \cdots & 1 \end{bmatrix},$$

$$R = \begin{bmatrix} 1 & 0 & \cdots & 0 \\ 1 & 1 & \cdots & 0 \\ \vdots & \vdots & & \vdots \\ 1 & 1 & \cdots & 1 \end{bmatrix}.$$
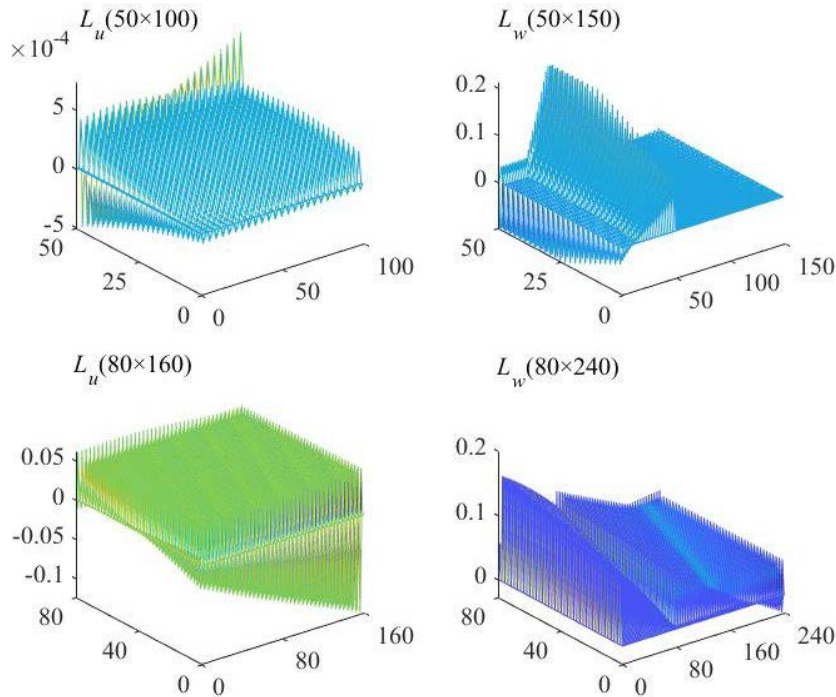
FIGURE 4. Subspace matrices L_u and L_w.

D. IDENTIFICATION OF SUBSPACE IDENTIFICATION MODEL AND VERIFICATION OF THE TRADITIONAL DATA-DRIVEN PREDICTIVE CONTROLLER

In this section, an identification and verification of subspace identification model is presented and a few simulations are performed to verify the emission optimization effects of the traditional data-driven predictive controller with fixed subspace identification model. The simulation is conducted in MATLAB/Simulink environment utilizing an Intel(R) Core(TM) i7-10700 CPU (2.90GHz).

1) IDENTIFCATION AND VERIFCATION OF SUBSPACE IDENTIFICATION MODEL

The identification data of the SCR system (as shown in Fig. 3) under the WHTC cycle with cold-initial engine are adopted, which come from the high-precision model in our previous work [29]. They consist of four inputs ($NO_{x,in}$, $NH_{3,in}$, T_{engine}, EF_M) and two outputs ($NO_{x,out}$, $NH_{3,out}$), which has 1650 seconds with a sampling time of 0.1 seconds. And, the two outputs are calibrated by the control strategy of the original ECU in accordance with the China/Euro VI emission regulations.

The normalized input and output data are used to derive the L_u and L_w matrices by the identification method described above, that is, the subspace identification model is obtained. As shown in Fig. 4, Two sets of matrices $L_u = 50 \times 100, L_w = 50 \times 150$ and $L_u = 80 \times 160, L_w = 80 \times 240$ are derived to compare the predicted accuracy.
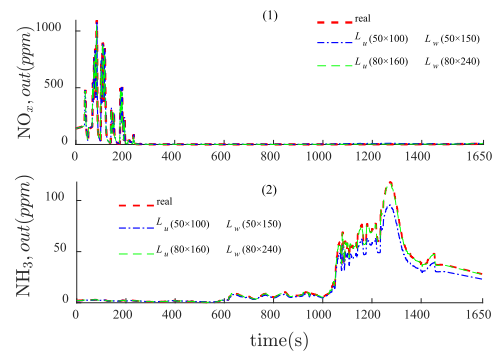

FIGURE 5. Predicted results of subspace identification model under the WHTC cycle with cold-initial engine: (1) $NO_{x,out}$, (2) $NH_{3,out}$.

As shown in Fig. 5, when the input data are the same, the comparison between the identification data (Real marked by red solid line) and the predicted data of subspace identification model is performed. When the dimension of L_u is 50×100 and L_w is 50×150, the predicted accuracy of the subspace identification model for $NO_{x,out}$ and $NH_{3,out}$ are 90.17% and 74.23%, respectively. When the dimension of L_u is 80×160 and L_w is 80×240, the predicted accuracy of the subspace identification model for $NO_{x,out}$ and $NH_{3,out}$ are 97.84% and 96.23%, respectively. Its predicted accuracy can satisfy the test requirements of the control system.
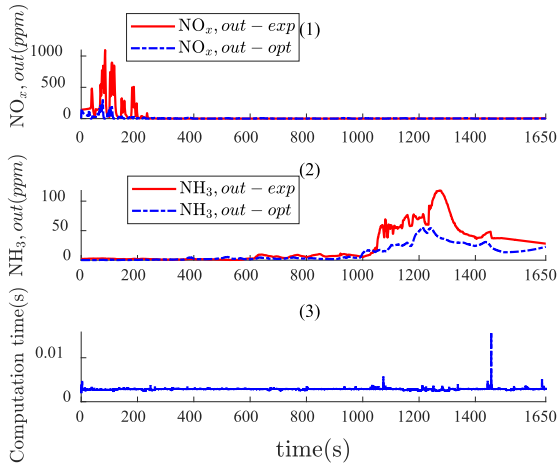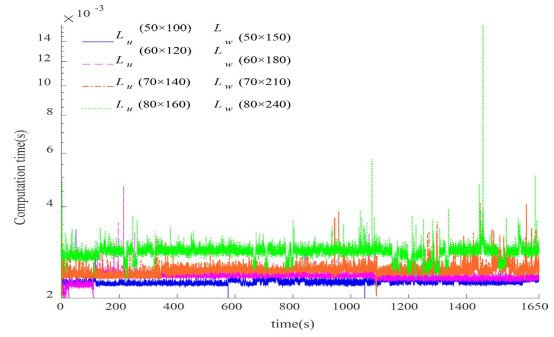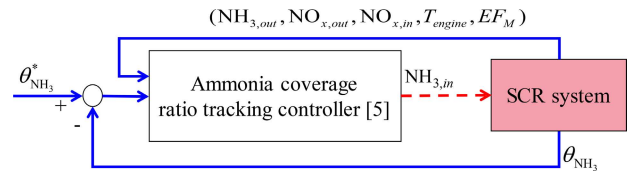
FIGURE 6. Comparison results of the emission control between the identification data controlled by the original ECU and optimized data controlled by the traditional data-driven predictive controller under the WHTC cycle with cold-initial engine: (1) $NO_{x,out}$, (2) $NH_{3,out}$, (3) computation time.
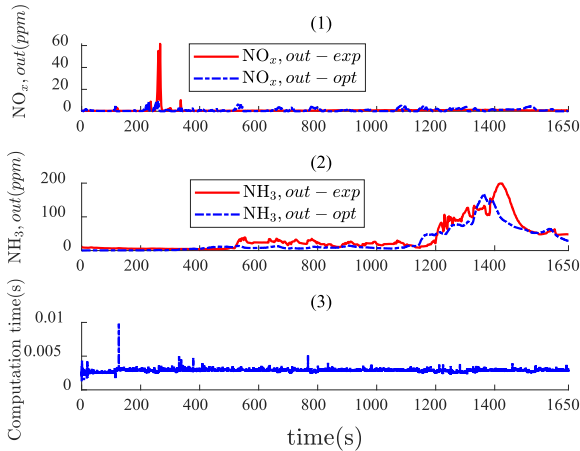
FIGURE 7. Comparison results of the emission control between the identification data controlled by the original ECU and optimized data controlled by the traditional data-driven predictive controller under the WHTC cycle with hot-initial engine: (1) $NO_{x,out}$, (2) $NH_{3,out}$, (3) computation time.

2) VERIFICATION OF THE TRADITIONAL DATA-DRIVEN PREDICTIVE CONTROLLER

In this subsection, a few simulation comparisons of the NO_x and NH_3 emissions are performed under the WHTC cycle with cold-initial and hot-initial engine, respectively. The emission optimization effects of the traditional data-driven predictive controller with $L_u = 80 \times 160$, $L_w = 80 \times 240$ are verified through the comparisons with the identification data of $NO_{x,out}$ and $NH_{3,out}$ controlled by the original ECU. As shown in Fig. 6, the emission comparisons between the identification data ($NO_{x,out} - exp$ and $NH_{3,out} - exp$) and optimized data ($NO_{x,out} - opt$ and $NH_{3,out} - opt$) controlled by the traditional data-driven predictive controller are performed under the WHTC cycle with cold-initial engine.

FIGURE 8. Comparison results of the computation times under the different dimensions of the subspace matrices

FIGURE 9. Schematic of tracking controller for the ammonia coverage ratio.

As compared to those of the identification data controlled by the original ECU, the average NO_x and NH_3 emissions of the traditional predictive controller are improved by 75.10% and 66.40%, respectively. The worst computation time of the traditional data-driven predictive controller is approximately 0.016 s with an average 0.0028 s. The worst computation time exceeds the reasonable real-time computation time (0.01 s).

As shown in Fig. 7, the emission comparisons between the identification data and optimized data controlled by the traditional data-driven predictive controller are performed under the WHTC cycle with hot-initial engine to verify its generality and robustness. As compared to those of the original ECU, the average NO_x and NH_3 emissions of the traditional predictive controller are improved by −0.93% and 25.79%, respectively. The worst computation time of the traditional data-driven predictive controller is approximately 0.0098 s with an average 0.0028 s.

E. COMPARSION AND DISCUSSION OF THE COMPUTATION TIMES

The computation time of the predictive controller is affected by the complexity of the subspace identification method, which is determined by the dimension of the subspace matrices. As shown in Fig. 8, under the WHTC cycle with cold-initial engine the computation times of the traditional data-driven predictive controller are compared, whose subspace matrices L_w and L_u are divided into four different dimensions. When the dimension of L_u is 50×100 and L_w is 50×150, the average computation time of the predictive controller saves a 17.86% compared with that of the controller when L_u is 80×160 and L_w is 80×240. The reduced
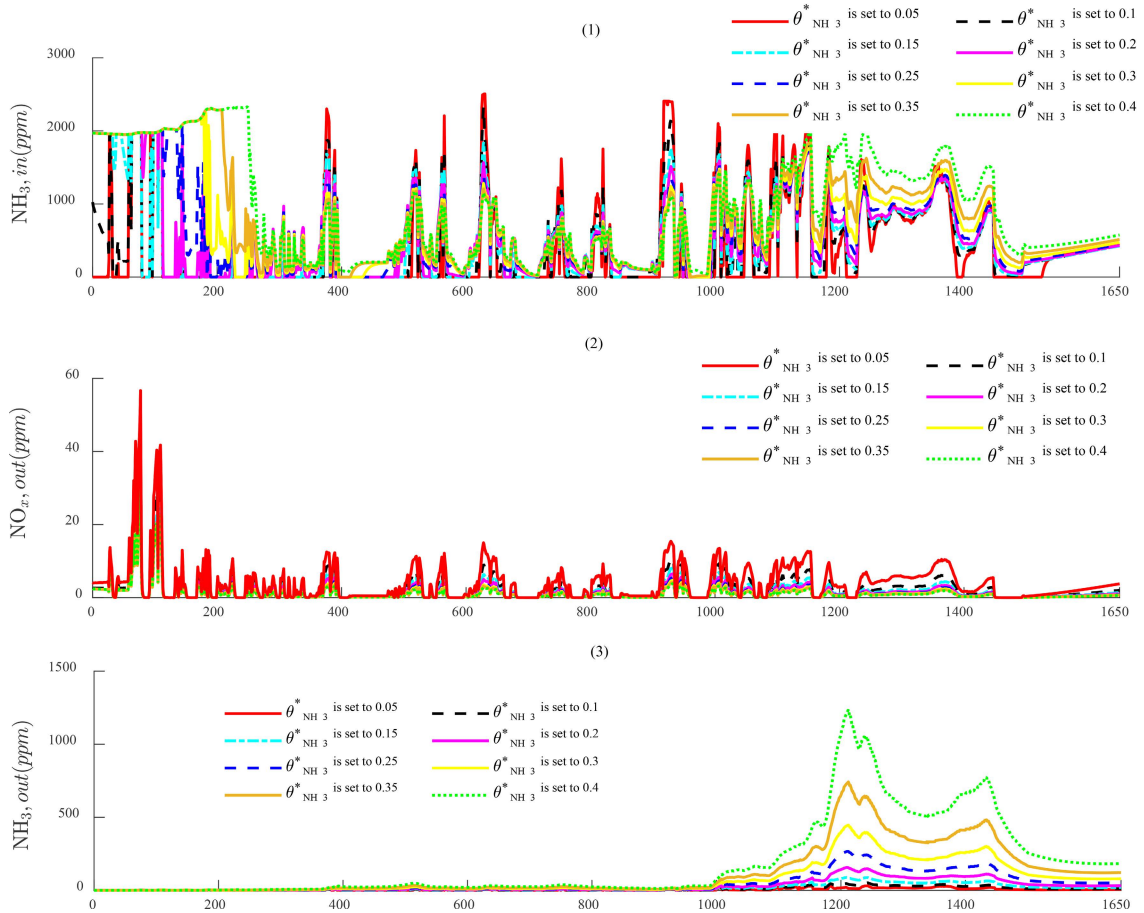
FIGURE 10. Updated input and output data by the different tracking target of the ammonia coverage ratio: (1) $NH_{3,in}$, (2) $NO_{x,out}$, (3) $NH_{3,out}$.

dimension of the subspace matrices will inevitably lead to a decrease in model accuracy. In the following sections, a segmented identification model excited by the segmented data will be discussed to guarantee model accuracy, and a corresponding predictive control method is proposed.

IV. PROPOSED DATA-DRIVE PREDICTIVE CONTROLLER WITH SWITCHED SUBSPACE MATRICES

In this section, a novel identification method for some lower order subspace matrices excited by the segmented data is established, and a corresponding data-driven predictive controller is designed and verified.

A. IDENTIFCARION OF SEGMENTED SUBSPACE MODEL REFERRING TO THE DYNAMIC OF THE AMMONIA COVERAGE RATIO

In this subsection, subspace matrices are excited by the segmented data referring to the dynamic of the ammonia coverage ratio. For obtaining the segmented data, a tracking controller of the ammonia coverage ratio [5] is employed,
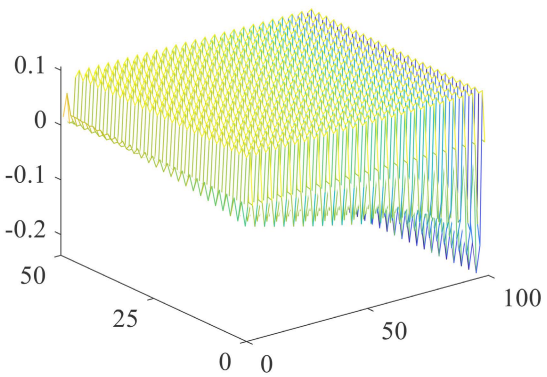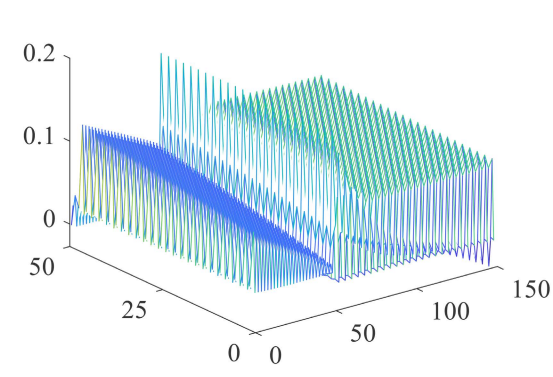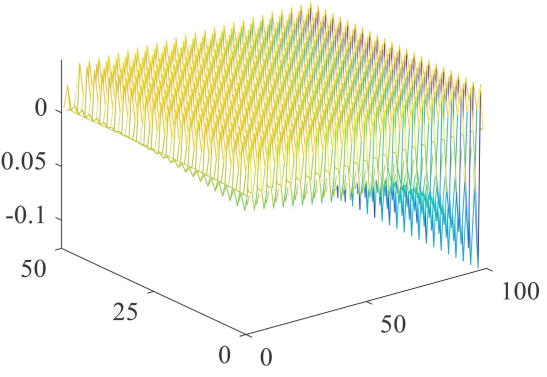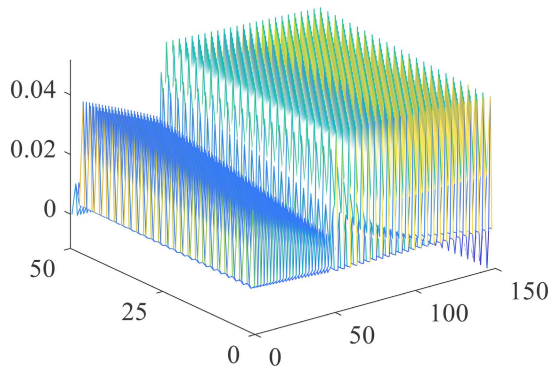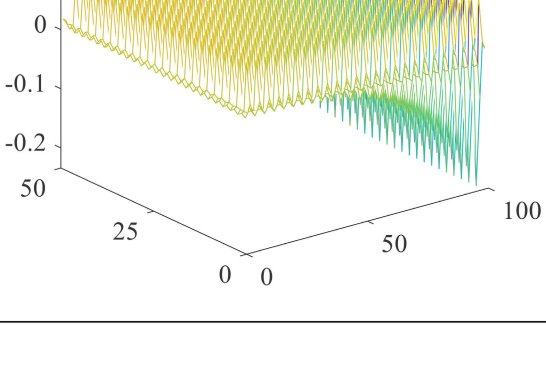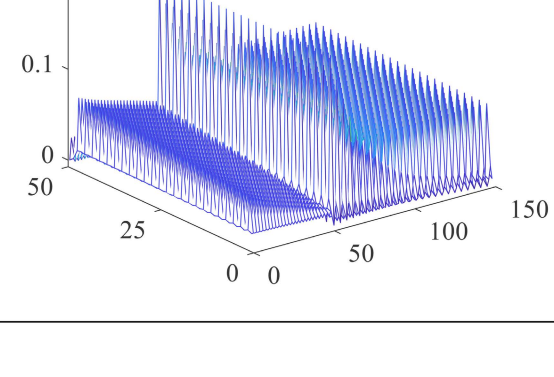
which controls $NH_{3,in}$ for tracking the target of the ammonia coverage ratio $\theta^*_{NH_3}$, as shown in Fig. 9.

Under the same working conditions ($NO_{x,in}$, T_{engine} and EF_M), several sets of segmented data for $NH_{3,in}$, $NO_{x,out}$ and $NH_{3,out}$ are obtained by the controller tracking the different $\theta^*_{NH_3}$. The target $\theta^*_{NH_3}$ are set to 0.05, 0.1, 0.15, 0.2, 0.25, 0.3, 0.35 and 0.4, respectively, and 8 sets of segmented data collected are shown in Fig. 10. Subspace matrices L_u and L_w excited under the different $\theta^*_{NH_3}$ are shown in Tab. 1.

B. VERIFCATION OF THE PROPOSED DATA-DRIVEN PREDICTIVE CONTROLLER

In this subsection, based on the previous segmented subspace matrices a data-driven predictive controller with the switched subspace matrices according to the dynamic of the ammonia coverage ratio is designed. The switched regulation of the subspace matrices is described as Eq. (17). The input data collected of the proposed controller includes θ_{NH_3}. When $0 < \theta_{NH_3} < 0.075$, L_w is assigned L_{w1}, and L_u is assigned L_{u1}. Similarly, when θ_{NH_3} takes values in

TABLE 1. Subspace matrices L_u with the dimension of 50 × 100 and L_w with the dimension of 50 × 150 excited under THE different tracking targets of the ammonia coverage ratio.

$\theta^*_{NH_3}$	L_u	L_w
0.05	L_{u1}	L_{w1}
0.1	L_{u2}	L_{w2}
0.15	L_{u3}	L_{w3}

TABLE 1. *(Continued.)* Subspace matrices L_u with the dimension of 50 × 100 and L_w with the dimension of 50 × 150 excited under THE different tracking targets of the ammonia coverage ratio.

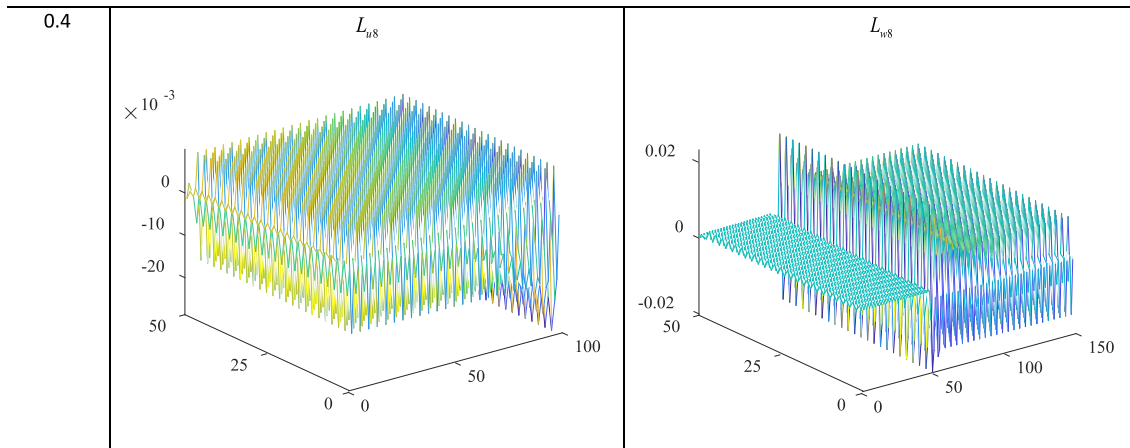| 0.2	L_{u4}	L_{w4}
0.25	L_{u5}	L_{w5}
0.3	L_{u6}	L_{w6}
0.35	L_{u7}	L_{w7}
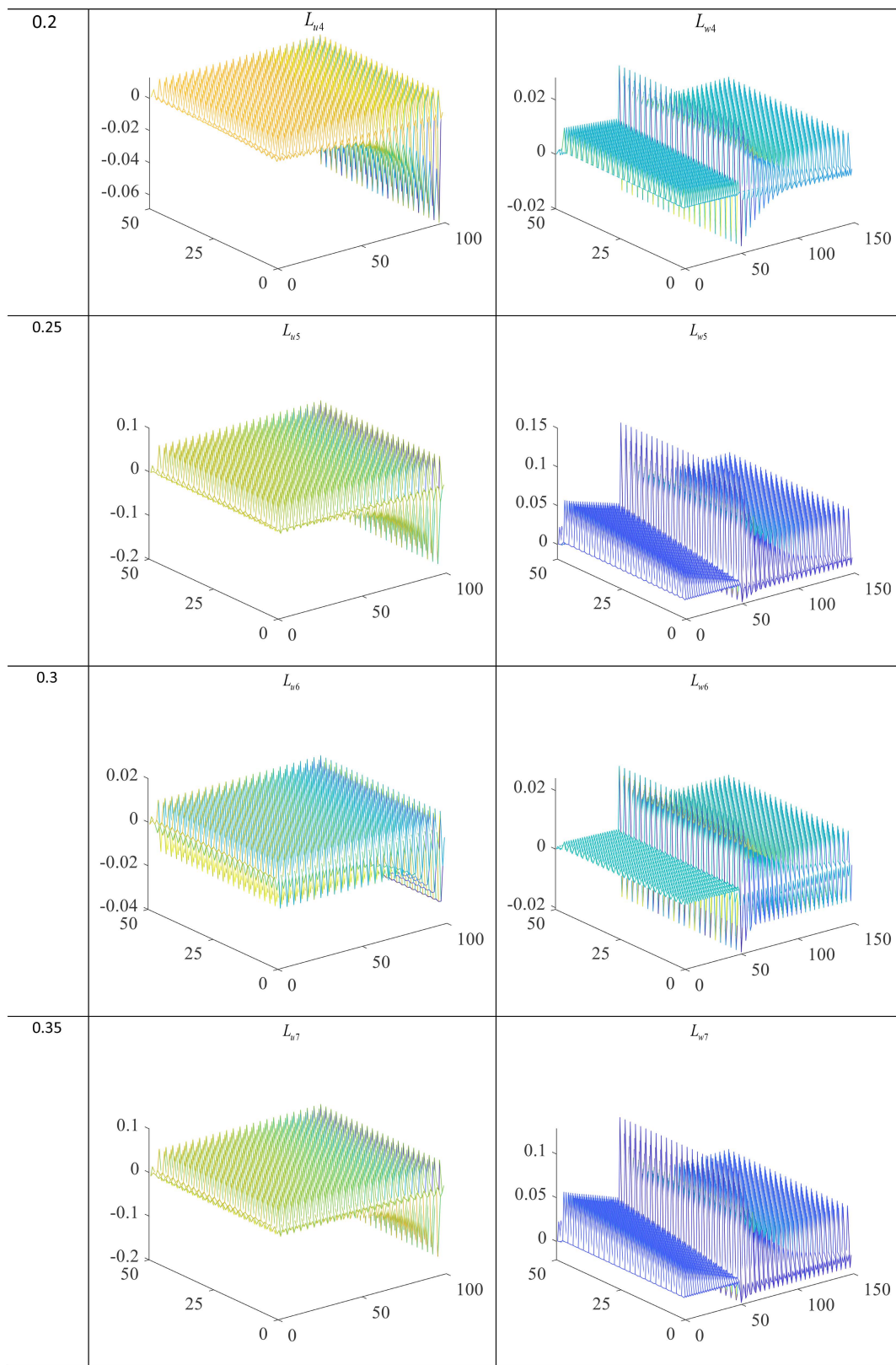
TABLE 1. *(Continued.)* Subspace matrices L_u with the dimension of 50 × 100 and L_w with the dimension of 50 × 150 excited under THE different tracking targets of the ammonia coverage ratio.


different ranges, L_w switches between $L_{w1}, L_{w2}, \ldots, L_{w8}$, and L_u switches between $L_{u1}, L_{u2}, \ldots, L_{u8}$. Based on the current L_w and L_u, the proposed controller starts to calculate.

$$
L_w \; L_u = \begin{cases} L_{w1} & L_{u1} & when & 0 < \theta_{\mathrm{NH_3}} < 0.075 \\ L_{w2} & L_{u2} & when & 0.075 \le \theta_{\mathrm{NH_3}} < 0.125 \\ L_{w3} & L_{u3} & when & 0.125 \le \theta_{\mathrm{NH_3}} < 0.175 \\ L_{w4} & L_{u4} & when & 0.175 \le \theta_{\mathrm{NH_3}} < 0.225 \\ L_{w5} & L_{u5} & when & 0.225 \le \theta_{\mathrm{NH_3}} < 0.275 \\ L_{w6} & L_{u6} & when & 0.275 \le \theta_{\mathrm{NH_3}} < 0.325 \\ L_{w7} & L_{u7} & when & 0.325 \le \theta_{\mathrm{NH_3}} < 0.375 \\ L_{w8} & L_{u8} & when & 0.375 < \theta_{\mathrm{NH_3}} \end{cases}
$$

(17)

The proposed data-driven predictive controller with the switched subspace matrices is verified under the WHTC cycle with cold-initial and hot-initial engine, respectively. As shown in Fig. 11, the emission comparisons between the identification data ($\mathrm{NO}_{x,out} - exp$ and $\mathrm{NH}_{3,out} - exp$) and optimized data ($\mathrm{NO}_{x,out} - opt$ and $\mathrm{NH}_{3,out} - opt$) controlled by the proposed data-driven predictive controller are performed under the WHTC cycle with cold-initial engine. As compared to those of identification data controlled by the original ECU, the average NO_x and NH_3 emissions of the proposed data-driven predictive controller are improved by 81.13% and 66.31%, respectively. The worst computation time of the proposed data-driven predictive controller is approximately 0.0034 s with an average 0.0023 s. Moreover, the average NO_x and NH_3 emissions of the traditional predictive controller mentioned in section III are improved by 75.10% and 66.40%, respectively. The worst computation time of it is approximately 0.016 s with an average 0.0028 s. As compared to those of the traditional controller, the average NO_x and NH_3 emissions of the proposed data-driven predictive controller are improved by 6.03% and −0.09%, the worst and average computation time are improved by 0.0126 s and 0.0005 s.
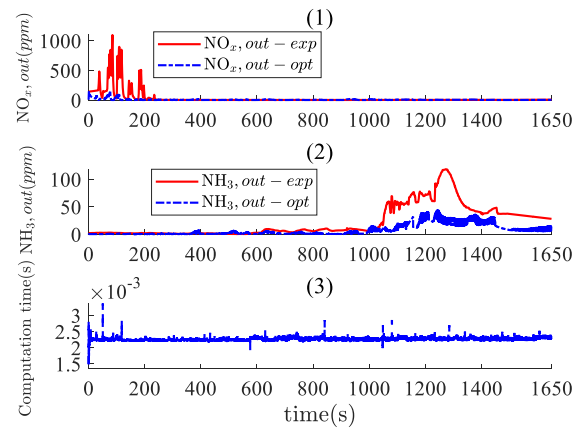
FIGURE 11. Comparison results of the emission control between the identification data controlled by the original ECU and optimized data controlled by the proposed data-driven predictive controller under the WHTC cycle with cold-initial engine: (1) $\mathrm{NO}_{x,out}$, (2) $\mathrm{NH}_{3,out}$, (3) computation time.

As shown in Fig. 12, the emission comparisons between the identification data and optimized data controlled by the proposed data-driven predictive controller are performed under the WHTC cycle with hot-initial engine to verify its generality and robustness. As compared to those of the identification data, the average NO_x and NH_3 emissions of the proposed data-driven predictive controller are improved by 2.71% and 31.46%, respectively. The worst computation time of the proposed data-driven predictive controller is approximately 0.0031 s with an average 0.0023 s. Moreover, the average NO_x and NH_3 emissions of the traditional predictive controller mentioned in section III are improved by −0.93% and 25.79%, respectively. The worst computation time of it is approximately 0.0098 s with an average 0.0028 s. As compared to those of the traditional controller, the average NO_x and NH_3 emissions of the proposed predictive controller are improved by 3.64% and 5.67%, the worst and average computation time are improved by 0.0067 s and 0.0005 s. Under the non-identification condition of the WHTC cycle
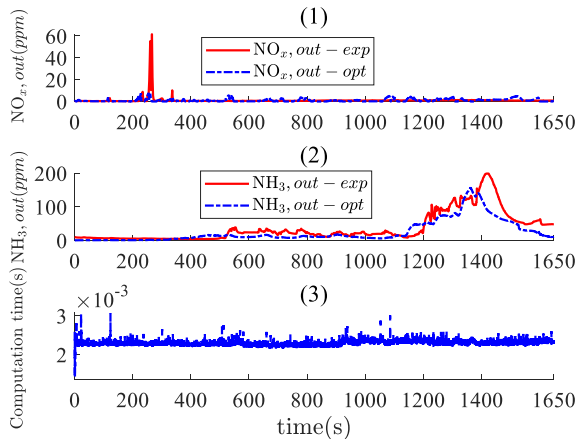
FIGURE 12. Comparison results of the emission control between the identification data controlled by the original ECU and optimized data controlled by the proposed data-driven predictive controller under the WHTC cycle with hot-initial engine: (1) $NO_{x,out}$, (2) $NH_{3,out}$, (3) computation time.

with hot-initial engine, the proposed data-driven predictive controller can also improve the emissions and computation time, and its optimization effects have better robustness to uncertainties of the transient cycle.

V. CONCLUSION

To simultaneously achieve high NO_x conversion efficiency and low NH_3 slip, this paper presents a data-driven predictive controller with switched subspace matrices for an SCR system. The segmented identification method for some lower order subspace matrices excited by the segmented data referring to the dynamic of the ammonia coverage ratio is established. The corresponding predictive controller with the switched subspace matrices according to working conditions is designed in order to further improve its real-time performance, generality and robustness. The simulation results show that under the identification condition of the WHTC cycle with cold-initial engine the proposed predictive controller compared to those of the traditional method can improve the average emission amount of NO_x and NH_3 by 6.03% and −0.09% and reduce the worst and average computation time by 0.0126 s and 0.0005 s, that under the non-identification condition of the WHTC cycle with hot-initial engine the proposed predictive controller compared to those of the traditional method can also improve the average emission amount of NO_x and NH_3 by 3.64% and 5.67% and reduce the worst and average computation time by 0.0067 s and 0.0005 s. Our future work will focus on using real-time calculation methods to solve the optimization problems, and performing experimental verification for the control strategy proposed in this paper.

REFERENCES

[1] J. Zhao, X. Gong, Y. Hu, J. Gao, and H. Chen, "An ammonia coverage ratio observing and tracking controller: Stability analysis and simulation evaluation," *Sci. China Inf. Sci.*, vol. 62, no. 6, Jun. 2019, Art. no. 062201.

[2] H. Zhang, P. Chen, J. Wang, and Y.-Y. Wang, "Integrated study of inland-vessel diesel engine two-cell SCR systems with dynamic references," *IEEE/ASME Trans. Mechatronics*, vol. 22, no. 3, pp. 1195–1206, Jun. 2017.

[3] P. Chen and J. Wang, "Coordinated active thermal management and selective catalytic reduction control for simultaneous fuel economy improvement and emissions reduction during low-temperature operations," *J. Dyn. Syst., Meas., Control*, vol. 137, no. 12, pp. 634–641, Dec. 2015.

[4] J. H. Zhao, Y. F. Hu, and B. Z. Gao, "Sequential optimization of eco-driving taking into account fuel economy and emissions," *IEEE Access*, vol. 4, pp. 130841–130853, 2019.

[5] J. Zhao, Y. Hu, X. Gong, and H. Chen, "Modelling and control of urea-SCR systems through the triple-step non-linear method in consideration of time-varying parameters and reference dynamics," *Trans. Inst. Meas. Control*, vol. 40, no. 1, pp. 287–302, 2018.

[6] J. Zhao, S. Zhou, Y. Hu, M. Ju, R. Ren, and H. Chen, "Open-source dataset for control-oriented modelling in diesel engines," *Sci. China Inf. Sci.*, vol. 62, no. 7, Jul. 2019, Art. no. 077201.

[7] S. Lespinats, M. Verleysen, A. Giron, and B. Fertil, "DD-HDS: A method for visualization and exploration of high-dimensional data," *IEEE Trans. Neural Netw.*, vol. 18, no. 5, pp. 1265–1279, Sep. 2007.

[8] H. Chen and F. Allgöwer, "A quasi-infinite horizon nonlinear model predictive control scheme with guaranteed stability," *Automatica*, vol. 34, no. 10, pp. 1205–1217, Oct. 1998.

[9] W. Favoreel and B. D. Moor, "SPC: Subspace predictive control," Dept. Electr. Eng., Katholieke Universiteit, Leuven, Brussels, Belgium, Tech. Rep. ESAT-SISTA/TR 1998-49, 1998, pp. 49–98.

[10] C. Gao, L. Jian, X. Liu, J. Chen, and Y. Sun, "Data-driven modeling based on Volterra series for multidimensional blast furnace system," *IEEE Trans. Neural Netw.*, vol. 22, no. 12, pp. 2272–2283, Dec. 2011.

[11] A. Kusiak, Z. Song, and H. Zheng, "Anticipatory control of wind turbines with data-driven predictive models," *IEEE Trans. Energy Convers.*, vol. 24, no. 3, pp. 766–774, Sep. 2009.

[12] X. Yin, S. Li, J. Wu, N. Li, W. Cai, and K. Li, "Data-driven based predictive controller design for vapor compression refrigeration cycle systems," in *Proc. 9th Asian Control Conf. (ASCC)*, Jun. 2013, pp. 1–6.

[13] J. Y. Ye, "Data-driven based predictive control design for temperature of molten pool during LASCR additive manufacturing," Ph.D. dissertation, College Mech. Transp. Eng., Hunan Univ., Changsha, China, 2016.

[14] J. Sun, "Research on optimal control strategy for hybrid electric vehicle driving system," Ph.D. dissertation, College Control Sci. Eng., Shandong Univ., Jinan, China, 2015.

[15] Y. N. Fan, "Data-driven based engine air-fuel ratio predictive," M.S. thesis, Jilin Univ., Changchun, China, 2014.

[16] Y. F. Hu, Y. T. Ding, and Z. X. Zhao, "Data-driven modeling and receding optimization control of diesel engine combustion process," *J. Jilin Univ. Eng. Technol. Ed.*, vol. 51, no. 1, pp. 49–62, 2021.

[17] X. Lu, H. Chen, P. Wang, and B. Gao, "Design of a data-driven predictive controller for start-up process of AMT vehicles," *IEEE Trans. Neural Netw.*, vol. 22, no. 12, pp. 2201–2212, Dec. 2011.

[18] X. Lu, H. Chen, B. Gao, Z. Zhang, and W. Jin, "Data-driven predictive gearshift control for dual-clutch transmissions and FPGA implementation," *IEEE Trans. Ind. Electron.*, vol. 62, no. 1, pp. 599–610, Jan. 2015.

[19] J. Y. Bai, X. J. Lei, and Y. X. Hu, "Modeling of denitration system using the particle swarm algorithm with adaptive weights," *Process Autom. Instrum.*, vol. 40, no. 5, pp. 13–17, 2019.

[20] Z. Dong and L. Q. Yan, "Modelling and simulation for NO_x emission concentration of SCR denitrification system," *J. Syst. Simul.*, vol. 32, no. 2, pp. 172–181, 2020.

[21] J. H. Zhao, Y. F. Hu, and H. T. Liu, "Design of data-driven predictive controller for urea injection of urea-SCR systems," *Trans. Chin. Soc. Agricult. Machinery*, vol. 49, no. 1, pp. 366–374, 2018.

[22] J. Xiang, X. Du, Y. Wan, Y. Chen, J. Ran, and L. Zhang, "Alkali-driven active site shift of fast SCR with NH_3 on V_2O_5–WO_3/TiO_2 catalyst via a novel Eley–Rideal mechanism," *Catal. Sci. Technol.*, vol. 9, no. 21, pp. 6085–6091, 2019.

[23] X. Wang, B. Huang, and T. Chen, "Data-driven predictive control for solid oxide fuel cells," *J. Process Control*, vol. 17, no. 2, pp. 103–114, Feb. 2007.

[24] P. Van Overschee and B. D. Moor, "A unifying theorem for three subspace system identification algorithms," *Automatica*, vol. 31, no. 12, pp. 1853–1864, Dec. 1995.

[25] R. Kadali, B. Huang, and A. Rossiter, "A data driven subspace approach to predictive controller design," *Control Eng. Pract.*, vol. 11, no. 3, pp. 261–278, Mar. 2003.

[26] D. He, H. Li, and H. Du, "Lexicographic multi-objective MPC for constrained nonlinear systems with changing objective prioritization," *Automatica*, vol. 125, Mar. 2021, Art. no. 109433.

[27] J. Luo, D. He, W. Zhu, and H. Du, "Multiobjective platooning of connected and automated vehicles using distributed economic model predictive control," *IEEE Trans. Intell. Transp. Syst.*, early access, May 4, 2022, doi: 10.1109/TITS.2022.3170977.

[28] K. Lu, S. Mizuno, and J. Shi, "A new mixed integer programming approach for optimization over the efficient set of a multiobjective linear programming problem," *Optim. Lett.*, vol. 14, no. 8, pp. 2323–2333, Nov. 2020.

[29] Y. Sun, Y. F. Hu, J. M. Zhou, and J. H. Zhao, "Moving horizon optimization control of SCR system based on hierarchical controller," *J. Jilin Univ. Eng. Technol. Ed.*, to be published, doi: 10.13229/j.cnki.jdxbgxb20210596.
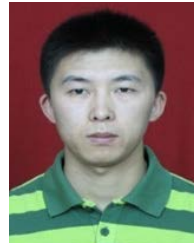
YUNFENG HU received the M.S. degree in basic mathematics and the Ph.D. degree in control theory and control engineering from Jilin University, Changchun, China, in 2008 and 2012, respectively. He is currently a Professor with the Department of Control Science and Engineering, Jilin University. His current research interests include nonlinear control and automotive control.

JINGHUA ZHAO received the M.S. degree in software engineering from the Harbin Institute of Technology, Harbin, China, in 2008, and the Ph.D. degree in power machinery and engineering from Jilin University, Changchun, China, in 2012. He is currently an Associate Professor with the Computer College, Jilin normal University. His current research interests include nonlinear control and automotive control.

JIE LIU received the B.S. degree in computer science and technology from Jilin Normal University, Siping, China, in 2020, where she is currently pursuing the master's degree with the Computer College. Her current research interests include data modeling and artificial intelligence.

YAO SUN received the B.S. degree in thermal energy and power engineering and the M.S. and Ph.D. degrees in power machinery and engineering from Jilin University, Clhangchun, China, in 2011, 2014, and 2018, respectively. From 2018 to 2021, he held a postdoctoral position in control science and engineering at Jilin University. Since 2022, he has been an Associate Professor with the State Key Laboratory of Automotive Simulation and Control, Changchun. His research interests include vehicle emissions reduction and intelligent automotive powertrains.

HONGYU SUN received the Ph.D. degree from Jilin University, Changchun, China, in 2017. From January 2015 to September 2016, she was a Visiting Scholar with the University of Maryland, Baltimore County. Currently, she is an Assistant Professor with Jilin Normal University. She has published over 20 articles in SCI/EI international conference proceedings and journals. Her research interests include wireless communication and mobile computing, RF-based sensing, privacy and security, and the Internet of Things (IoT).

FANGXI XIE received the M.S. and Ph.D. degrees in power machinery and engineering from Jilin University, Changchun, China, in 2007 and 2010, respectively. He is currently a Professor with the Automotive Engineering College, Jilin University. His current research interests include high-efficiency vehicle power system development and key component design.

· · ·